# NJC

Accepted Manuscript


This is an *Accepted Manuscript*, which has been through the Royal Society of Chemistry peer review process and has been accepted for publication.

*Accepted Manuscripts* are published online shortly after acceptance, before technical editing, formatting and proof reading. Using this free service, authors can make their results available to the community, in citable form, before we publish the edited article. We will replace this *Accepted Manuscript* with the edited and formatted *Advance Article* as soon as it is available.

You can find more information about *Accepted Manuscripts* in the Information for Authors.

Please note that technical editing may introduce minor changes to the text and/or graphics, which may alter content. The journal's standard Terms & Conditions and the Ethical guidelines still apply. In no event shall the Royal Society of Chemistry be held responsible for any errors or omissions in this *Accepted Manuscript* or any consequences arising from the use of any information it contains.

ROYAL SOCIETY OF CHEMISTRY

www.rsc.org/njc

Cite this: DOI: 10.1039/c0xx00000x

www.rsc.org/xxxxxx

ARTICLE TYPE

# Studying the emission complexity of the conjugated molecules through manipulating the molecular aggregate state

**Fu-yin Wang,[a] Ying-hui Wang,*[a,b] Ning Sui,[a] Yun-fei Song,[c] Yu-guang Ma[b] and Han-zhuang Zhang*[a]**

***Received (in XXX, XXX) Xth XXXXXXXXX 20XX, Accepted Xth XXXXXXXXX 20XX***

**DOI: 10.1039/b000000x**

We prepare the quantum dot (QD) based on conjugated molecules (Coumarin 6, C-6), which is considered to be mesoscopic aggregate, to build a bridge linking monodisperse state (solution state) and macroscopic aggregate (powders state). Their spectral features involving steady spectral data, dynamic feature and fluorescence quantum yield have been compared in detail. All dynamic data are modelled by continuous rate distribution function. The final result shows that fluorescence quantum yield of organic quantum dots based on C-6 gradually decreases as the QD's size increases, which may be assigned to the enhancement of nonaradiative relaxation rate originated from the aggregation. It is beneficial for people to further understand the optical characteristics of the conjugated molecules.

## Introduction:

Conjugated organic luminescence species have been demonstrated in a wide range of optoelectronic device application[1,2]. Many conjugated organic light emitters own high fluorescence quantum yield in their dilute solutions, but their luminescence becomes quenched when fabricated into thin films[3] or powders. In the solid state, the molecules easily aggregate to form less emissive species such as excimers or are influenced by nonradiative relaxation path, which decreases the luminescence yield[4]. Therefore, the decrease of fluorescence quantum yield originated from aggregation could strongly influence the application of organic conjugated luminescence species. Up to now, people devote much attention to investigate the optical characteristics of conjugated molecules. Due to the limitation of previous condition, people mainly focused on the conjugated molecules in solution or bulk aggregation state (such as powder and film). These aggregation states normally belong to amorphous state and have complex morphologies, where the molecules could orderly arrange in short range and in-orderly arrange in large scales. Due to absence of a bridge between the monodisperse state (solution state) and macroscopic aggregate (powder or film), the emission evolution of conjugated molecule from solution to aggregated state still remains unclear and need to be further analyzed.

Recently, people develop a popular technique to prepare quantum dots (QDs) based on organic molecules, and the corresponding operation is easy and versatile[5]. The rapid addition of a very dilute conjugated materials solution is added into a nonsolvent, usually water, and this mixed solution results in a sudden decrease of solvent quality, which induces precipitation of the conjugated materials. Finally the QD based on conjugated molecules could be obtained and the size of organic QD could be easily tailored via the concentration of the organic material solution. In this situation, the organic QD shows many novel photophysical characteristics[6,7] and they could be considered to be a mesoscopic aggregate according to its scale. Through tailoring the organic QDs (manipulating the size of QD), people could build a bridge linking the monodisperse state (solution state) and the macroscopic amorphous state (films or powders), which is beneficial to observe the evolution process of conjugated molecule's photophysical properties.

In this paper, we prepared seven kinds of samples based on conjugated molecules (C-6), They are C-6 ethanol solution, five C-6 QDs with different size, and C-6 powders. They covers the monodisperse state, mesoscopic aggregate and macroscopic aggregate, and could be used to observe the aggregate-dependent spectral characteristics of conjugated molecules. Based on the decay rate distribution model, the variance of fluorescence dynamic information at different aggregates is also further analyzed.

## Experimental:

The C-6 ethanol solution is named #1 with concentration of 1000 μM. Two kinds of C-6 QDs with different sizes are prepared based on reference 8 and they were obtained through mixing the water and ethanol solution of C-6 with concentration of 5 (#2), 50 (#3), 100 (#4), 150 (#5), 250 (#6) μM. The ratio between water and ethanol is 3:1. The diameter distribution of #2, #3, #4, #5 and #6 are detected by Malvern Zetasizer Nano ZS (Marven, zen3600). The C-6 powder is named #7, which is obtained from thick C-6 ethanol solution after the evaporation of ethanol solvent. Steady-state absorption measurements were carried out using a UV–Vis spectrophotometer (Purkinje, TU-1810PC). Photoluminescence (PL) spectra were recorded by a fiber optic spectrometer (Ocean Optics, USB4000) with

excitation pulse at 400 nm. For the emission dynamic investigations, a picoseconds laser system (Becker & Hickl GmbH, BDL-375-SMC) with a repetition rate of 20 MHz was employed to excite samples. The photoluminescence originated from samples was passed through monochromator (Zolix, SSM101) and detected by single photon detection module (id Quantique, id100-50), which is connected with Time-Correlated Single Photon Counting (TCSPC) measurement card (Becker & Hickl GmbH, SPC-130) at personal computer. All the measurements are operated at room temperature.

## Results and discussion

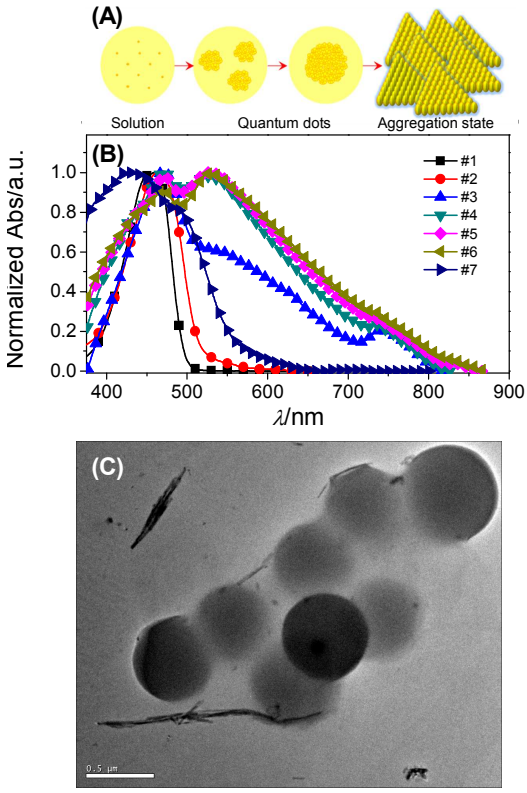


**Figure 1**: (A) Scheme of C-6 molecules in different aggregation state; (B) normalized absorption spectra of #1 (C-6 in ethanol solution), #2~#6 (C-6 QDs with different diameters and #7 (C-6 powders); (C) TEM image of #4.

We illustrate the evolution of molecular aggregate in Fig. 1(A). In the C-6 solution (#1), molecular interaction does not appear among C-6 molecules. When the C-6 molecules form the QDs in mixed solution (#2~#6), the short range molecular interaction appears in aggregation state under mesoscopic scale. If the C-6 molecules in the bulk amorphous state (#7), the molecular interaction is much complex, which could influence the photophysical properties of C-6. The normalized absorption spectra of all samples (#1~#7) are shown in Figure 1(B). The absorption maximum of #1~#6 shows a gradual red-shift behavior. Meanwhile, we offer the TEM image of #4, showing that the shape of organic QDs based on C-6 molecules is closed to sphere and the diameter is estimated to be about ~500 nm. In order to clarify the size distribution of these organic QDs (#2 ~ #6) in detail, their size distributions are shown in Figure 2. Apparently, the size of QDs gradually increases. According to the Figure 1(B) and Figure 2, it is interesting found that the intermolecular interaction among conjugated molecules gradually enhances with the increasing of the QD's scale, since the absorption spectra gradually red shift.

In addition, Figure 1(B) exhibits that the C-6 absorption band gradually posses discrete energy levels splits with the increasing of the QD's size, indicating that the intermolecular interaction could lead to the splitting of excited state. In addition, the stronger background scattering at wavelengths < 900 nm was assigned to the larger size of the aggregate. The strong Rayleigh scattering of a red laser pointer beam by a dispersion of the aggregates versus no visible Rayleigh scattering by the C-6 QDs is another proof of the existence of large aggregates. As the size of the QD increases, the scattering phenomenon become obviously. Therefore the absorption spectra of C-6 QDs gradually broaden as the size of C-6 QDs increases, as seen in Figure 1(B). However, the absorption maximum of #7 is located between those of #2 and #4. Considering the amorphous state of #7, we expect that the scale of aggregate in #7 is between that of #2 and #4, the short range interaction in #7 should affect its absorption spectrum. Apparently, these samples based on C-6 samples cover the monodisperse state, mesoscopic aggregation state (QDs with different sizes) and macroscopic aggregation state. The absorption shape of C-6 could be sensitive to the aggregate state of C-6 molecules.

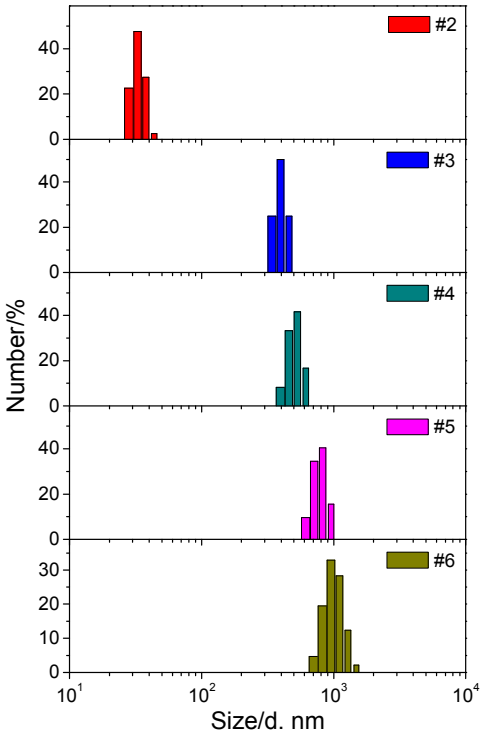


**Figure 2**: The size distribution of #2 ~ #6 (QD based on C-6 molecules) in mixed solution.

The normalized fluorescence spectra of C-6 QDs with different sizes are offered in Figure 3(A), showing that the fluorescence maximum of #2 ~ #6 also red shift as the size of QDs increases, which is in agreement with the tendency of previous absorption data. Meanwhile, the emission spectrum of

C-6 solution is in the blue side, since the molecule interaction could disappear in the solution. However, it is interesting found that the fluorescence maximum of #7 is also located between that of #2 and #4, indicating that the short range interaction could affect the fluorescence of conjugated molecules simultaneously. The excitation intensity-dependent fluorescence integrated intensity of #1, #2, #4 and #7 are exhibited in Figure 3(B), and are fitted by using function of $I_{FI} \propto I_E^{\alpha}$, where the $I_{FI}$ and $I_E$ are fluorescence integrated intensity and the excitation intensity, respectively. Finally, we found that $\alpha$ of #1 and #2 is closed to 1, indicating that no fluorescence loss happens at high intensities. But $\alpha$ of #4 is ~0.973 and less than 1, which should be assigned to the annihilation of exciton or excimers[3] at high concentration as C-6 together aggregated. In #7, $\alpha$ is ~0.956, indicating that the exciton or excimer's annihilation based on collision could further enhanced at high excitation intensity, when C-6 molecules in powder state. In addition, we also measured the fluorescence quantum yields of #1 ~ #6, and summarized in inset of Fig. 3(B). Apparently, the fluorescence quantum yield (FQY) of conjugated molecules in QDs could gradually decrease and tend to a constant (~0.1), as the size of QDs increases.

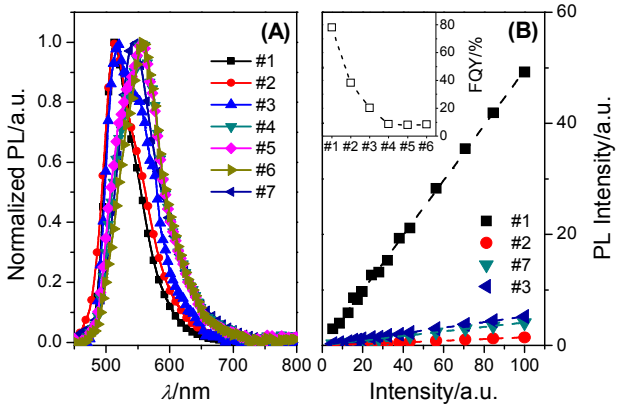


**Figure 3:** (A) Normalized emission spectra of #1~#7; (B) the excitation intensity-dependent fluorescence integrated intensity of #1, #2, #4 and #7. Inset: the corresponding fluorescence quantum yields of #1 ~ #7.

In Figure 3(A), we exhibit fluorescence decay traces of all samples based on C-6 molecules. Considering their complex and non-exponential decay behaviors, all the fluorescence decay traces are fitted with a continuous rate distribution model[9]:

$$I(t) = I(0)\int_{\gamma=0}^{\infty} \varphi(\gamma)\exp(-\gamma t)\,d\gamma \quad (1)$$

where $\varphi(\gamma)$ is the distribution of decay rates with dimension of time; $I(t)$ is the fluorescence intensity; $\varphi(\gamma)$ is the distribution function[10] as described below:

$$\varphi(\gamma) = A\exp\left(-\ln^2(\gamma/\gamma_{MF})/w^2\right) \quad (2)$$

where $\gamma_{MF}$ is the most-frequency decay rate corresponding to the maximum of $\varphi(t)$; $w$ is a dimensionless width parameter that determines the distribution width ($\Delta\gamma$) at $1/e$; $A$ is the normalization constant, so that $\int\varphi(\gamma)d\gamma = 1$. $\gamma_{MF} = k_{nonrad} + k_{rad}$, which is determined by the non-radiative and radiative rates. The fitted lines are shown in Figure 3(A) with solid lines and the corresponding rate-distribution functions are summarized in Figure 3(B). Meanwhile, the distribution width could be calculated as described below:

$$\Delta\gamma = 2\gamma_{MF}\sinh w \quad (3)$$

Herein, $\gamma_{MF}$ of C-6 are 0.395 (#1), 0.539 (#2), 0.543 (#3), 0.549 (#4), 0.554 (#5), 0.558 (#6) and 0.732 $ns^{-1}$ (#7), and the width ($\Delta\gamma$) of their distribution function is 0.122 (#1), 0.409 (#2), 0.415 (#3), 0.422 (#4), 0.429 (#5), 0.434 (#6) and 1.353 $ns^{-1}$ (#7). The FQY of conjugated molecules could be calculated based on function of FQY = $k_{rad}/(k_{rad}+k_{nonrad})$. Compared with dynamic traces and the FQY of #1 and #2, we expect that the acceleration of $k_{nonrad}$ in #2 should mainly be assigned to the influence of intermolecular interaction among C-6 in #2. The dynamic relaxation process of #3 is similar to that of #2, but the FQY of #3 is much lower than that of #2 (as seen inset of Figure. 2(B)), indicating that that the $k_{nonrad}$ of C-6 could further accelerate if the aggregate degree gradually enhances. Apparently, the nonardiative relaxation rate is sensitive to the size of organic QDs and able to reach an extremum with the increasing of QD's size, which leads to the saturation of FQY as seen inset of Figure 3(B). For the fluorescence decay traces of #7, its dynamic behavior is much complex and its $\gamma_{MF}$ obviously enhances in comparison with those of #2~#6 (C-6 QD). Since the molecular interaction among C-6 in amorphous state contains the long range interaction and the short range interaction, it is expected that the long range interaction could be responsible for the further enhancement of $\gamma_{MF}$ in #7. Since the chemical environment of C-6 amorphous state become complex and the intermolecular interactions have multi-forms, $\gamma_{MF}$ of #7 obviously accelerates and the corresponding width ($\Delta\gamma$) become broad.

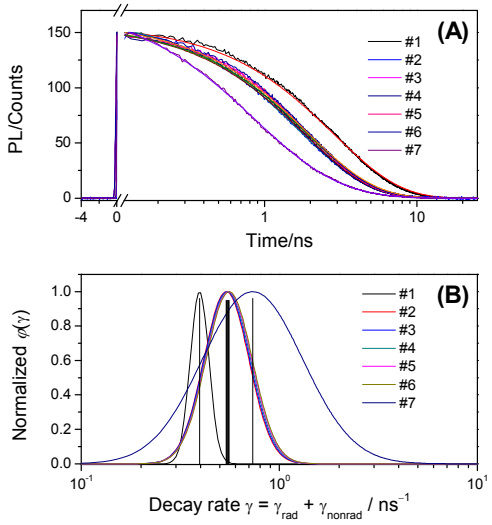


**Figure 4**: (A) Fluorescence decay traces of #1~#7; (B) their corresponding decay-rate distributions $\varphi(\gamma)$ and $\gamma_{MF}$. $\gamma_{MF}$ of C-6 are 0.395

(#1), 0.539 (#2), 0.543 (#3), 0.549 (#4), 0.554 (#5), 0.558 (#6) and 0.732 $ns^{-1}$ (#7), and the width ($\Delta\gamma$) of their distribution function are 0.122 (#1), 0.409 (#2), 0.415 (#3), 0.422 (#4), 0.429 (#5), 0.434 (#6) and 1.353 $ns^{-1}$ (#7).

## Conclusions

We observed the steady and dynamic spectral features of conjugated molecules (C-6) in different chemical environment, which covers simple monodisperse state (solution), mesoscopic aggregate (QD), and complex macroscopic amorphous state (powder). We found that the intermolecular interaction could appear after molecule aggregate together and become complex as the scale of aggregate gradually increases, which could make the optical properties of conjugated molecules become complex. The final results could be beneficial for people to further understand the optical characteristics of conjugated molecules in aggregate.

## Acknowledgement

This work was supported by the National Natural Science Foundation of China (Nos. 21103161, 11274142 and 11304058), and the China Postdoctoral Science Foundation (2011M500927 and 2013T60319).

## Notes and references

[a] *Femtosecond Laser Laboratory, College of Physics, Jilin University, Changchun 130012, People's Republic of China*

[b] *State Key Laboratory of Supramolecular Structure and Materials, Jilin University, Changchun 130012, People's Republic of China*

[c] *Department of Physics, Harbin Institute of Technique, Harbin 150000, China.*

1 M. Gross, D. C. Muller, H. G. Nothofer, U. Scherf, D. Neher, C. Brauchle, K. Meerholz, *Nature. 2000, **405**, 661.*

2 P. Peumans, A. Yakimov, S. R. Forrest. *J. Appl, Phys. 2003, **93**, 3693.*

3 R. H. Friend, R. W. Gymer, A. B. Holmes, J. H. Burroughes, R. N. Marks, C. Taliani, D. D. C. Bradley, D. A. Dos. Santos. J. H. Bredas, M. Logdlund, W. R. Salaneck, *Nature. 1999, **397**, 121.*

4 S. A. Jenekhe, J. A. Osaheni, *Science 1994, **265**, 765.*

5 B.-K. An, S.-K. Kwo, S.-D. Jung, S. Y. park,*J. Am. Chem. Soc. 2002, **124**, 14410.*

6 D. Horn, J. Rieger. Angew. Chem., *Int. Ed. 2001, **40**, 4330.*

7 G.J.Bhogale,C.-W.Chang,E.W.-G.Diau,C.-S.Hsu,Y.Dong,B.-Z.Tang, *Chemical Physics Letters,2006,**419**,444.*

8 C. F. Wu, C. Szymanski, J. McNeill, *Langmuir. 2006, **22,** 2956.*

9 I. S. Nikolaev, P. Lodahl, A. F. van Driel, A. F. Koenderink, *W. L.* Vos,*Phys. Rev. B 2007, **75**, 115302*.

10 A. F. van Driel, I. S. Nikolaev, P. Vergeer, P. Lodahl, D. Vanmakekelbergh, *W. L. Vos. Phys. Rev. B 2007, **75**, 035329*.

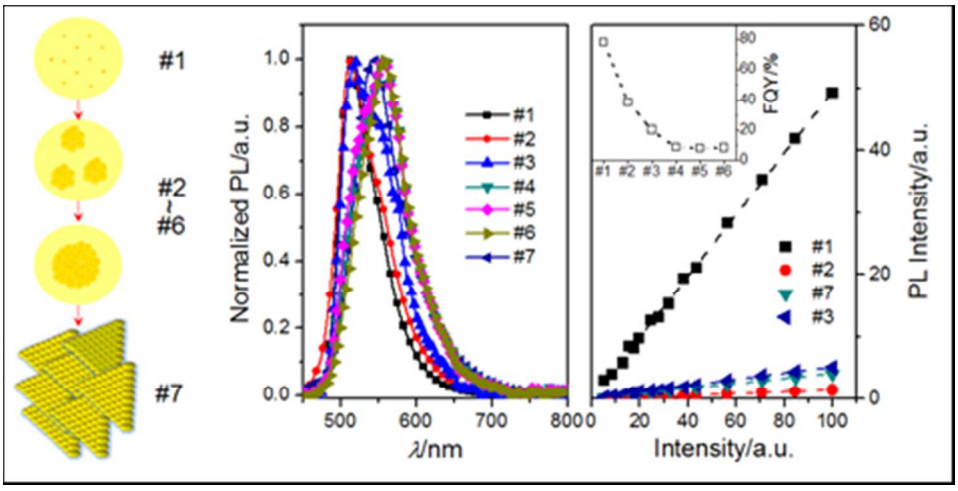


80x40mm (150 x 150 DPI)